The frequency deviation and filter bandwidth for the system were determined, not by the bit rate but by the LD spectral spread. Therefore, the bit rate could be increased to 140 Mbit/s with the same experimental set-up, and a high receiver sensitivity of −54·1 dBm ($P_e = 10^{-9}$) has been achieved.

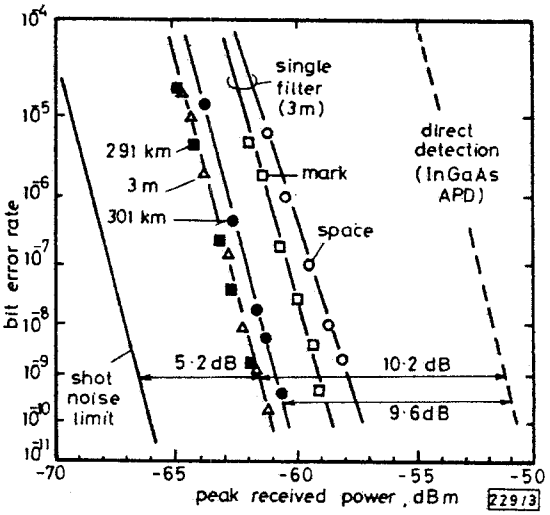

Fig. 3 *Error rate against peak received signal level characteristics after long-span transmission*

P_{LO} = 2·3 dBm, 34 Mbit/s

A 291 km transmission experiment has been carried out at 34 Mbit/s, using the balanced receiver. The receiver sensitivity showed no degradation after transmission. Furthermore, by increasing the transmitter LD bias level, a 301 km transmission experiment has been successfully carried out. Power levels and device characteristics in the 301 km transmission experiment are summarised in Table 1. In this case, the transmitter DFB LD oscillated in two modes with a 20:1 power ratio. As the receiver sensitivity shows a 0·6 dB degradation due to this two-mode oscillation, a large-span loss margin of 66·9 dB has been achieved, which results in a 1·3 dB margin after 301 km transmission.

Table 1 POWER LEVELS AND DEVICE CHARACTERISTICS

Transmitter LD (phase-tunable DFB LD):	
Output power	11·7 dBm
Fibre input power	7·1 dBm
Spectral linewidth (FWHM)	10 MHz
Frequency shift	500 MHz
Local oscillator LD (DFB LD):	
Output power	7 dBm
Total receiver input power	2·3 dBm
Spectral linewidth (FWHM)	10 MHz
Relative intensity noise	−155 dB/Hz
Fibre (21 drums with splices):	
Length	301 km
Loss (at 1·545 μm)	65·6 dB
Coupler:	(0·218 dB/km)
Coupling ratio	1:0·9
Excess loss	1 dB
Receiver sensitivity ($P_e = 10^{-9}$)	−61·4 dBm
after 301 km transmission	−60·8 dBm
Margin	1·3 dB
Span loss margin	66·9 dB

Conclusion: An over 300 km transmission experiment has been successfully carried out on a 34 Mbit/s optical FSK heterodyne dual filter detection system. High-power phase-tunable DFB LDs and high-sensitivity (−61·4 dBm) dual filter detection with the balanced receiver contribute greatly to the long-span transmission.

Acknowledgments: We would like to thank M. Sakaguchi, F. Saito, K. Washio and K. Kobayashi for encouragement during the course of the work. We are also grateful to our colleagues for supplying the optical devices.

K. EMURA
S. YAMAZAKI
S. FUJITA
M. SHIKADA
I. MITO
K. MINEMURA

Opto-Electronics Research Laboratories
NEC Corporation
4-1-1 Miyazaki, Miyamae-ku
Kawasaki 213, Japan

19th August 1986

References

1 YAMAZAKI, S., EMURA, K., SHIKADA, M., YAMAGUCHI, M., MITO, I., and MINEMURA, K.: 'Long-span optical FSK heterodyne single-filter detection transmission experiment using a phase-tunable DFB laser diode', *Electron. Lett.*, 1986, **22**, pp. 5–7

2 YAMAZAKI, S., EMURA, K., SHIKADA, M., YAMAGUCHI, M., and MITO, I.: 'Realisation of flat FM response by directly modulating a phase-tunable laser diode', *ibid.*, 1985, **21**, pp. 283–285

3 KASPER, B. L., BURRUS, C. A., TALMAN, J. R., and HALL, K. L.: 'Balanced dual-detector receiver for optical heterodyne communication at Gbit/s rates', *ibid.*, 1986, **22**, pp. 413–415

OPTICAL ACTIVATION OF A SILICON VIBRATING SENSOR

Indexing terms: Semiconductor devices and materials, Measurement, Silicon

The operation of a micromachined silicon vibrating sensor with both optical excitation and optical interrogation is reported. The proper locations at which the optical excitation should be applied for optimum excitation of different modes of resonance are described.

Introduction: Micromachined silicon mechanical resonators are attractive for sensor applications because of their frequency output. This provides immunity to fluctuations of the intensity of the signal and easy interfacing with digital systems. The full optical operation of these devices, i.e. both optical excitation and optical interrogation, is an important objective that will increase reliability and safety by avoiding any electromagnetic interference. Optical fibres and micromachined silicon resonators are nicely compatible in size and the combination should lead to rugged and successful sensor systems.

A sensitive interferometric optical fibre technique has already been reported* for interrogating the vibrations of a micromachined silicon pressure sensor. In those experiments the vibrations were excited piezoelectrically, but this has recently been successfully replaced by direct optical powering of the resonator. A few bulk optical components are still used, but the actual set-up could easily be converted into a full optical fibre arrangement.

Venkatesh and Culshaw[1] have previously reported the optical excitation of the vibrations of a light silica beam ($200 \times 5 \times 1\ \mu m^3$), and this letter reports similar optical excitation of a relatively large silicon resonator ($1000 \times 125 \times 8\ \mu m^3$) designed specifically as a sensor in this case a pressure sensor.[2] Several resonances have been detected using an average optical power within the range 0·1 to 1 mW. The amplitudes of the vibrations that are actually excited are a few nanometres, but some experiments are in progress to improve the coupling efficiency of the optical power.

Experimental arrangement: Fig. 1*a* shows a diagram of the pressure transducer. The mechanical resonator consists of two rectangular arms connected by an elastic junction, and each is supported by two V supports on to two ribs which are inte-

gral with the 8 μm-thick diaphragm. When a pressure difference exists across the diaphragm, it will distort and induce a stress on the V supports. This stress will determine the actual value of the frequency of resonance. The way in which the sensor is mounted (Fig. 1*b*) allows a vacuum operation, and

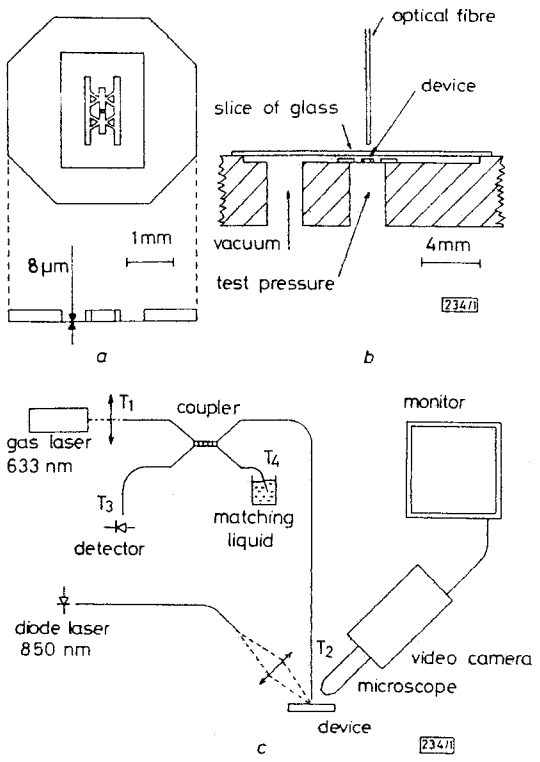

Fig. 1

a Pressure transducer
b Holder
c Experimental arrangement

therefore high Q-factors can be achieved. At the same time a test pressure can be applied to the bottom of the diaphragm, and a calibration of the device can be performed.

Fig. 1*c* is a diagram of the whole set-up. Three parts can be distinguished: the interrogating system, the optical powering system and a video circuit. The interrogating system is interferometric and consists basically of a 3 dB single-mode coupler. The signal detected at T_3 is the interference between the reflection produced at the fibre/air interface at terminal T_2 and the light that is reflected by the resonator and coupled back into the fibre. This interferometric signal is a function of the distance between the fibre end and the resonator, and is independent of the environmental changes that can affect the optical length of the fibre. A CW laser diode (LC30 series, 0·850 μm) with a multimode fibre tail is used to power the resonator optically. The output of this fibre is focused on the resonator by a lens. The laser diode is driven to produce pulses of up to 2·25 mW and 2 μs, at a repetition frequency which can be tuned accurately to the appropriate resonant frequency. Finally, a video camera provides a magnified picture of the device and the two spots can be observed. The spot generated by the interrogating fibre is a few micrometres in diameter, the same size as the core of the single-mode fibre, and the spot of the powering light is about 60 μm in diameter. The position of each spot can be controlled independently.

Procedure and results: Each resonance has its own characteristic shape of vibration and it is known* at which point the amplitude of vibration is maximum. These points are clearly the best positions for the interrogating fibre. The distance between the fibre end and the resonator has to be adjusted to obtain the maximum sensitivity, corresponding to the two reflections being in quadrature at equilibrium.

Once the interrogating fibre is placed on an optimum position for the particular mode we want to investigate, the resonator is scanned by the powering spot of light. A map of the efficiency of the optical excitation can be deduced for each mode of resonance, and Fig. 2 summarises the results,

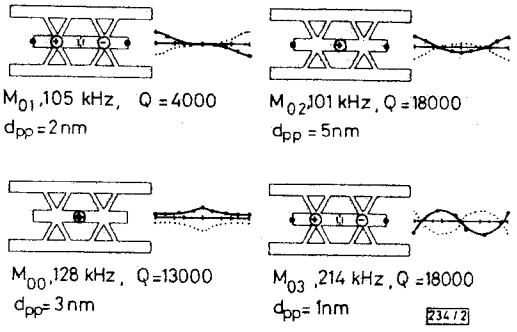

Fig. 2 *Maps of optical excitation and vibration shapes*

Test pressure is atmospheric pressure, d_{pp} = maximum peak-to-peak displacement detected
• optimum interrogating points
± regions of best efficiency of optical excitation and relative phase of vibration excited

showing the excitation regions for best efficiency. Some modes can be excited by focusing the powering signal on to the V supports and even on to the holding ribs. We have detected only the lowest four modes using optical excitation.

Discussion: The excitation of a mechanical resonance by means of pulses of light can be explained in terms of the generation of acoustic waves by the light source. Each resonance of a mechanical resonator can be described by means of the standing pattern of acoustic waves which fits the shape of vibration of the mode of resonance. The efficiency of the optical excitation will depend on two factors: the intensity and type of acoustic waves generated by the pulses of light, and the coupling between these acoustic waves and the standing pattern associated with the mechanical resonance.

The photoacoustic generation in silicon has been described in terms of a superposition of thermal and electronic strain effects.[3,4] Both effects cause an isotropic volume dilation, but with opposite sign. At the present stage of our investigation we cannot identify which mechanism produces the more important contribution to the results.

The mechanical resonator of our experiment is made of a thin sheet of silicon of about 8 μm thickness. As a consequence, the lowest vibrational modes (at frequencies of hundreds of kilohertz) are resonances of the lowest antisymmetrical Lamb mode, a flexural mode. This mode is a superposition of a shear wave and a compressional wave, and therefore each resonance will exhibit a standing pattern of volume dilation associated with the compressional wave. The efficiency of the optical powering will be determined by how closely the volume dilatation associated with this resonance is matched by the volume dilatation generated by the pulses of light. The regions of maximum volume dilatation in a flexural mode of vibration correspond to the regions of maximum curvature. At these points the volume diltation has maximum values, of opposite sign, on the upper and lower surfaces of the resonator, and goes through zero at the neutral plane. Because of the relatively large diffusion lengths of the thermal and electronic effects in our device, the excitation of the mechanical resonance is produced only through the differential effect between the volume diltations generated at the top and bottom of the sheet. This leads to the poor efficiency of the optical powering of the resonator in the present devices.

Fig. 2 shows the relationship between the vibration shape and the regions for maximum efficiency of the optical excitation for a number of modes. The pulses of light excite the maximum amplitude of vibration when they are focused on the regions of maximum curvature. In the M_{01} and M_{03} modes the phase of the vibrations at any chosen point of the resonator changes by π, relative to the optical driving pulse, depending on which of the two indicated excitation points the powering beam is focused on. This corresponds to the fact that the two arms exhibit opposite curvature at any given moment.

* ANDRES, M. V., FOULDS, K. W. H., and TUDOR, M. J.: 'Optical-fibre detection technique applied to silicon vibrating sensors', submitted to *J. Lightwave Technol.*

Conclusions: To improve the efficiency of the optical activation of a mechanical resonator, the photoacoustic generation has to be optimised. The present results show a clear relationship between the shape of vibration of a particular mode and the location for the point of excitation which produces the highest efficiency of the optical powering.

Acknowledgments: We are indebted to J. Greenwood and P. Hale of STL Technology Ltd. (Harlow) for the micromachined Si devices and some optical fibre components, and to J. Barnett of STC plc for financial help. Acknowledgment of financial support is made by MJT for a CASE studentship from the UK SERC [through STC Technology Ltd. (Harlow)].

M. V. ANDRES

Department of Electricity & Magnetism
University of Valencia
Valencia, Spain

K. W. H. FOULDS
M. J. TUDOR

Physics Department
University of Surrey
Guildford, Surrey GU2 5XH, United Kingdom

21st August 1986

References

1 VENKATESH, S., and CULSHAW, B.: 'Optically activated vibrations in a micromachined silica structure', *Electron. Lett.*, 1985, **21**, pp. 315–317
2 GREENWOOD, J.: 'Etched silicon vibrating sensor', *J. Phys. E (Sci. Instrum.)*, 1984, **17**, pp. 650–652
3 KINO, G. S., and STEARNS, R. G.: 'Acoustic wave generation by thermal excitation of small regions', *Appl. Phys. Lett.*, 1985, **47**, pp. 926–928
4 STEARNS, R. G., and KINO, G. S.: 'Effect of electronic strain on photoacoustic generation in silicon', *ibid.*, 1985, **47**, pp. 1048–1050

ANALYSIS OF SINGULAR SYSTEMS USING TAYLOR SERIES APPROACH

Indexing terms: Control theory, Taylor series, Singular systems

The Taylor series approach to the analysis of singular systems is considered. An example is given to demonstrate the use of this method.

Introduction: In the past decade orthogonal functions have been widely applied to the analysis of regular dynamic systems with some success. The particular orthogonal series used are Walsh,[2,3] block-pulse,[4,5] Laguerre[6] and Chebyshev.[7] More recently, Paraskevopoulos[7,8] has extended the orthogonal functions to analysis of singular systems.

The primary motivation of their methods is to obtain an algebraic technique for solving the equations of dynamic systems. In this letter an alternative approach called the Taylor series approach is introduced. This approach is not an orthogonal function; however, it can lead to a simple form, and more convenient computation.

Problem statement: Let us consider the system of the form

$$\begin{aligned} E\dot{x} &= Ax + Bu \\ x(0) &= x_0 \end{aligned} \tag{1}$$

where $x \in \mathscr{R}^n$, $u \in \mathscr{R}^m$ and E, A and B are constant matrices. If $\det E = 0$ then the system characterised by eqn. 1 is called a singular or generalised state-space system. These systems are encountered in many areas, such as electrical networks, singularly perturbed systems, composite systems etc. This problem has been studied and the following analytical results, analogous to those for the case of regular systems, are obtained[1] as

$$x(t) = \exp(E^D A t)E^D E q + E^D \int_0^t \exp[E^D A(t-\tau)]Bu(\tau)\,d\tau - (I - EE^D)\sum_{n=0}^{k-1}[EA^D]^n A^D B u^{(n)}(t) \tag{2}$$

where E^D and A^D are Drazin inverses[1] of E and A, respectively, q is an arbitrary constant vector and k is the index of E, defined as the smallest non-negative integer k such that

$$\text{rank } E^k = \text{rank } E^{k+1} \tag{3}$$

Note that eqn. 2 holds under the restrictions

$$EA = AE \qquad N(E) \cap N(A) = \{0\} \tag{4}$$

Further, if eqn. 4 is fulfilled, then eqn. 1 has a solution with $x(0) = x_0$, if and only if x_0 takes the form

$$x_0 = E^D E q - (I - EE^D)\sum_{n=0}^{k-1}[EA^D]^n A^D B u^{(n)}(0) \tag{5}$$

Suppose that eqn. 4 does not hold: a simple transformation is applied to eqn. 1 and solutions similar to those of eqn. 2 are derived.[1]

It is apparent that we have difficulty in finding the solution of eqn. 2. To overcome this difficulty, a Taylor series approach would be presented, which is on the basis of approximating $x(t)$ by a truncated series as follows:

$$\begin{aligned} x(t) &= Hf(t), f^T(t) \\ &= [f_0(t), f_1(t), f_2(t), \ldots, f_{r-1}(t)] \end{aligned} \tag{6}$$

where $f_0(t), f_1(t), \ldots, f_{r-1}(t)$ are basis functions and H is an $n \times r$ constant matrix to be calculated.

Method: It has been shown that basis functions have the following property:[9]

$$\int_0^t f(\tau)\,d\tau \simeq Pf(t) \qquad 0 \le t \le 1 \tag{7}$$

where P is an operational matrix of integration. Now, integrating eqn. 1 from 0 to t gives

$$Ex - Ex_0 = A\int_0^t x(\tau)\,d\tau + B\int_0^t u(\tau)\,d\tau \tag{8}$$

Let $u(t)$ be approximated by the following truncated series:

$$u(t) = Uf(t) \tag{9}$$

where U is an $m \times r$ known matrix.

Substituting eqns. 6 and 9 into eqn. 8, and invoking eqns. 7 and 8 may be obtained as

$$EHf(t) - Ex_0 = AHPf(t) + BUPf(t) \tag{10}$$

The second term in the above equation, Ex_0, may be denoted as

$$Ex_0 = EKf(t) \qquad K = [x_0, \underbrace{0, 0, \ldots, 0}_{(r-1)\text{ columns}}] \tag{11}$$

where K is an $n \times r$ matrix. Inserting eqn. 11 in eqn. 10, and equating coefficients of like $f_i(t)$ functions, one would obtain

$$EH - EK = AHP + BUP \tag{12}$$

or

$$AHP - EH = D \qquad D = -EK - BUP \tag{13}$$